frontiers | Frontiers in Marine Science

TYPE Original Research
PUBLISHED 16 August 2022
DOI 10.3389/fmars.2022.973694

OPEN ACCESS

EDITED BY
Fajin Chen,
Guangdong Ocean University, China

REVIEWED BY
Guisheng Song,
Tianjin University, China
Liyang Yang,
Fuzhou University, China
Chao Wang,
Guangdong Ocean University, China

*CORRESPONDENCE
Xuchen Wang
xuchenwang@ouc.edu.cn

SPECIALTY SECTION
This article was submitted to Marine Biogeochemistry, a section of the journal Frontiers in Marine Science

RECEIVED 20 June 2022
ACCEPTED 25 July 2022
PUBLISHED 16 August 2022

CITATION
Ding L, Shan S, Luo C and Wang X (2022) Distribution and microbial degradation of dissolved organic carbon in the northern South China Sea.
Front. Mar. Sci. 9:973694.
doi: 10.3389/fmars.2022.973694

Distribution and microbial degradation of dissolved organic carbon in the northern South China Sea

Ling Ding[1,2], Sen Shan[3], Chunle Luo[1] and Xuchen Wang[1]*

[1]Frontiers Science Center for Deep Ocean Multispheres and Earth System, and Key Laboratory of Marine Chemistry Theory and Technology, Ocean University of China, Qingdao, China, [2]School of Naval Architecture and Port Engineering, Shandong Jiaotong University, Weihai, China, [3]North China Sea Administration, Ministry of Natural Resources, Qingdao, China

Dissolved organic carbon (DOC) is the largest reduced carbon pool in the ocean, and it plays significant roles not only in the ocean carbon cycle but also in the control of many biogeochemical processes in the ocean. We present the concentrations and distribution of DOC in the northern South China Sea (SCS) and western North Pacific (NP) in the spring and summer seasons of 2015-2016 and 2019. Laboratory incubation bioassay experiments were also conducted to determine the microbiological respiration of DOC. In the SCS, the concentrations of DOC varied within a range of 38-95 μM, and the large spatial variations in DOC in the upper 100 m depth were influenced by a combination of factors, including primary production, terrestrial inputs from the Pearl River and the intrusion of the Kuroshio Current. The mesopelagic DOC distribution in the northern SCS basin was largely influenced by the physical mixing of upwelled deep water; however, biological processes were estimated to account for 6-20% of the modulation in DOC concentrations. Compared with the deep DOC levels in open ocean areas, a slightly excessive DOC concentration (~ 3-4 μM) was observed in the deep water of the SCS basin. Approximately 10-20% of the DOC was consumed by mesopelagic and/or deep water bacteria in the incubation bioassay experiments, and labile DOC was preferentially respired, resulting in decreased $\delta^{13}C$ and $\Delta^{14}C$ values of DOC.

KEYWORDS

carbon cycle, biogeochemistry, dissolved organic carbon, microbial degradation, South China Sea

Introduction

Dissolved organic carbon (DOC) is the largest exchangeable organic carbon pool (~ 662 Pg) in the ocean, equal in size to atmospheric inorganic carbon (Hansell et al., 2009). DOC plays important roles not only in the oceanic carbon cycle but also in supporting and controlling the microbial communities in the ocean (Hansell and

Carlson, 2001; Azam and Worden, 2004; Fenchel, 2008; Benner and Amon, 2015). Minor changes in the DOC pool could thus have a considerable impact on both the carbon cycle and biogeochemical processes in the marine system (Carlson et al., 2010; Nelson and Carlson, 2012; Benner and Amon, 2015; Druffel et al., 2016). The ultimate source of oceanic DOC is thought to be derived from *in situ* primary production that is directly linked to oceanic CO_2 systems (Carlson et al., 1998; Carlson and Hansell, 2015). The removal of DOC *via* microbial uptake is the dominant biological consumption mechanism in the ocean (Hansell et al., 2009; Carlson and Hansell, 2015). As a result, a delicate balance exists between the production and degradation of DOC in the oceanic water column, and the concentrations and distribution of DOC in the deep ocean have been found to be quite consistent (Hansell et al., 2009; Carlson and Hansell, 2015; Druffel et al., 2016; Druffel et al., 2021).

The most dynamic changes in DOC distributions are found in the euphotic zone of the ocean. High DOC concentrations (70-90 μM) have been widely observed in surface water (≤ 100 m) and are related to primary production. Labile DOC (LDOC) is mainly produced from extracellular release by phytoplankton, zooplankton excretion, solubilization and remineralization of particulate organic carbon (POC) (Hansell, 2013; Carlson and Hansell, 2015). After release, the majority of LDOC is rapidly consumed and turned over within hours to days, supporting heterotrophic microbial production and resulting in remains of inorganic constituents (such as CO_2 and nutrients) being suspended within the euphotic zone in the ocean (Carlson and Ducklow, 1996; Cherrier et al., 1996; Hansell, 2013; Carlson and Hansell, 2015). The magnitude of DOC accumulation and export in the euphotic zones of different oceanic regions is therefore ultimately derived from the uncoupling of DOC production and consumption processes. In highly productive regions with high nutrient supplies from upwelling, such as the Peru coast and California Current, high primary production results in high DOC generation and consumption rates (Kirchman et al., 1991; Zweifel et al., 1993; Ducklow, 1999). In contrast, in open ocean sites with low available nutrients, low primary production results in low DOC concentrations and low consumption rates (Carlson and Ducklow, 1996; Carlson et al., 1996; Ducklow, 1999).

It has been estimated that ~17% of new production globally could escape rapid microbial degradation and accumulate in the surface layer of the ocean as semilabile DOC (Hansell and Carlson, 1998). If this portion of the DOC pool is exported into the ocean interior, the majority of exported DOC could become available to microbes and be remineralized within the mesopelagic zone (Hansell et al., 2002; Carlson et al., 2004; Carlson et al., 2010). Instead, a significant fraction of DOC (~ 38 μM), termed refractory DOC resisting to microbial degradation, is present throughout the water column in the ocean. This refractory DOC, characterized by old ^{14}C ages (4,000-6,000 years), likely survives multiple ocean mixing cycles in the ocean (Druffel et al., 1992; Druffel et al., 2019). In fact, DOC in the ocean is a complex mixture comprising thousands of individual molecules, including carbohydrates, proteins, lipids and black carbon (Ziolkowski and Druffel, 2010; Riedel and Dittmar, 2014; Repeta, 2015). Researchers have observed that high molecular weight (HMW) components of DOC were more bioavailable and that carbohydrate-like and protein-like materials comprised younger DOC fractions, whereas low molecular weight (LMW) components and lipids in the oceanic DOC pool were more recalcitrant and were thousands of years old (Guo et al., 1996; Loh et al., 2004; Repeta and Aluwihare, 2006; Benner and Amon, 2015).

Numerous seawater incubation and field studies (spanning days to months) have been conducted to quantify the fate of accumulated DOC and further elucidate the mechanisms controlling the microbial degradation of DOC in the ocean (Carlson et al., 2004; Nelson and Carlson, 2012; Shen and Benner, 2020). Based on these studies, the molecular size and chemical composition of DOC, which are likely linked to its variable radiocarbon age (via $\Delta^{14}C$), appeared to be the primary controls on its bioavailability and degradation in the ocean (Walker et al., 2011; Walker et al., 2016; Shen and Benner, 2020). In addition to quantifying the removal of oceanic DOC, these experiments were also used as platforms to assess the transformation of DOC composition as well as the concomitant shifts in microbial community structures (Carlson et al., 2004; Liu et al., 2020; Varela et al., 2020). While these bioassay experiments focused on the microbial degradation of DOC and provided potential linkages between DOC utilization and microbial lineages, the variation in the $\Delta^{14}C$-DOC values (or radiocarbon ages) during DOC degradation is still enigmatic and only supposed, lacking direct evidence of simultaneous carbon isotope measurements of DOC (both $\delta^{13}C$-DOC and $\Delta^{14}C$-DOC).

The South China Sea (SCS) is one of the largest semienclosed marginal seas in the North Pacific Ocean, covering an area of approximately 3.5×10^6 km^2. A few studies have reported that the surface distribution and seasonal dynamics of DOC in the SCS are largely modulated by water circulation and physical mixing processes (Hung et al., 2007; Pan and Wong, 2015; Meng et al., 2017; Zhang et al., 2020). The carbon isotope (^{13}C and ^{14}C) measurements of DOC further suggested that the dynamics of the DOC pool were mainly controlled by diffusive mixing and intensified vertical motion, rapid water exchange through the Luzon Strait and good water mixing in the SCS basin (Ding et al., 2020). However, Wu et al. (2017) and Ma et al. (2022) observed a significant dependence of DOC on biological production using measured and model results. Despite these studies on the dynamics of DOC in the SCS, the nature of its microbial degradation has not been well studied, and knowledge of the

variations in DOC concentrations and the Δ^{14}C-DOC values concomitant with DOC removal is still limited.

In this paper, we present the results of our field investigation of the concentrations and distribution of DOC in the northern SCS and the western North Pacific (NP). This field investigation was combined with laboratory incubation bioassay experiments characterizing the concentration and carbon isotopic (^{13}C and ^{14}C) signatures to evaluate the biological and hydrodynamic controls on the distribution of DOC in the northern SCS and to identify changes in DOC concentration and isotopic values associated with DOC degradation at the Southeast Asian Time-series Study (SEATS) site in the SCS.

Methods

Study areas

The SCS has an average water depth of 1,350 m and a maximum water depth of ~ 5,000 m in the northeast region (Chen et al., 2001). It is connected to the open ocean only through the Luzon Strait, with a maximal sill depth of approximately 2,200 m, and to the East China Sea (ECS) through the shallow Taiwan Strait (~ 50 m) (Figure 1). The northern SCS has an extensive shelf and is influenced by the input of the Pearl River, which is the second largest river in China and ranks 17th in the world in terms of annual water discharge (Dai et al., 2014). The surface circulation in the SCS is driven by a seasonal monsoon influence, which is characterized by a cyclonic circulation gyre in the entire deep basin during the northeast monsoon prevailing in winter and a strong anticyclonic gyre mainly in the south and a weakened cyclonic gyre in the north during the southwest monsoon that prevailing in summer (Liu et al., 2002; Qu et al., 2006; Wang and Li, 2009). These basin-wide surface circulation gyres effectively isolate the interior SCS from the influence of land runoff. Moreover, the Kuroshio intrusion through the Luzon Strait located at the northeastern rim also has an important impact on the circulation in the northern SCS, which is stronger in winter and weaker in summer (Nan et al., 2015; Jiang et al., 2020). Under the influence of seasonal atmospheric and oceanic forcing, the oceanic biogeochemistry in the SCS varies in space and time.

Sample collection and processes

Water samples for DOC concentration analysis were collected from two stations (S4 and S5) in the northern SCS during a summer cruise in July 2015 onboard R/V *Shiyan 3*, from 11 stations (A1, 2A1, A3, A6, A8, A10, K4, G2, F1, Y1 and SEATS) covering the northern shelf-slope-basin regions of the SCS during a spring-summer cruise in May-June 2016 onboard R/V *Dongfanghong-2* and from six stations (C06, C09, C16, C20, C26 and C28) nearby the Luzon Strait during a summer cruise in July August 2019 onboard R/V *Haida* (Figure 1). Among these

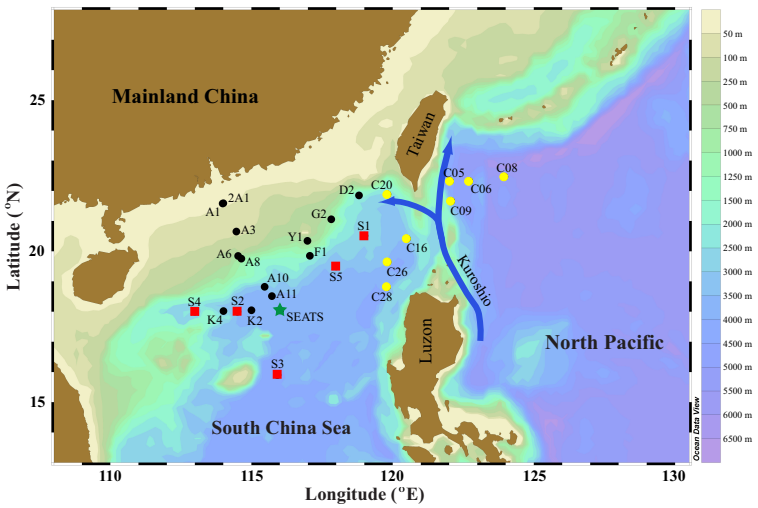

FIGURE 1
Map showing the study region and the locations of sampling stations in the northern SCS and western NP during three cruises in 2015 (red squares), 2016 (black circles) and 2019 (yellow circles), as described in the text. Seawater samples used for the incubation bioassay experiments were collected at the SEATS site (green star) during the cruise in May-June 2016. The blue arrows are the Kuroshio Current and its branching path into the SCS. Sampling stations in the SCS and western NP, from which published data were used for data validation in this paper, are also shown: S1, S2 and S3 (red squares) from the same cruise in 2015; D2, A11 and K2 (black circles) from the same cruise in 2016; and C05 and C08 (yellow circles) from the same cruise in 2019 (Ding et al., 2020). This map was created with Ocean Data View (ODV) (Schlitzer, 2017).

sampling stations, SEATS (18.3 °N and 115.5 °E) is the Southeast Asian time-series study site established in 1999, at which primary production and the carbon cycle have been extensively studied in recent decades. Water samples from these stations were collected using 5 L or 12 L Niskin bottles deployed on a rosette with a calibrated conductivity-temperature-depth (CTD) recorder that recorded the depth profiles of temperature and salinity. The CTD was calibrated at the National Center of Ocean Standards and Metrology in China (NCOSM) before the cruises and were within the calibration term of validity. In addition, large volumes of seawater (4-13 L) from the surface layer (5 m) and at 700 m and 1,500 m depths were collected at the SEATS site during the cruise in May-June 2016 for incubation bioassay experiments as described below.

After collection, water samples for DOC concentration analysis were transferred directly into a 1 L precombusted (550°C for 4 h) glass bottle that was first rinsed three times with seawater. The water was filtered immediately through Whatman GF/F filters (~ 0.7 μm, precombusted at 550°C for 4 h) on board. The filtered seawater was then acidified with super high purity 85% H_3PO_4 to pH ≤ 2 and preserved frozen at -20°C for analysis in the laboratory.

DOC incubation experiments

Previous studies have demonstrated that the surface water DOC that was originally resistant to degradation could be available to the mesopelagic microbial assemblage in the open ocean (Carlson et al., 2004; Nelson and Carlson, 2012; Shen and Benner, 2020). To test this in the SCS, we conducted incubation experiments by mixing filtered and unfiltered seawater from different depth at the SEATS site to evaluate the removal of DOC and simultaneous changes in the isotopic composition of bulk DOC. The designation of the experiments was based on Carlson et al. (2004). Briefly, surface seawater (5 m) was filtered with 0.22 μm Millipore polycarbonate filtrate (rinsed with the same seawater) to remove bacteria and then mixed separately with unfiltered mesopelagic (700 m) or deep (1500 m) seawater at a ratio of 2:1 (volume/volume). The mixed seawater in each experiment was well shaken and incubated with O_2 in the dark at room temperature (~26°C) for 180 days. Both incubations were conducted in duplicates. Samples for DOC concentration analysis were taken at various incubation time intervals (25-40 days) throughout the experiments by draining seawater directly from the incubation carboys into precombusted glass vials to prevent potential contamination. In addition, seawater samples for Δ^{14}C-DOC and δ^{13}C-DOC measurements were collected at the beginning and end of the experiments.

DOC concentration and isotope measurements

The DOC concentrations were analyzed by the high-temperature catalytic oxidation method (Sharp et al., 1995) using a Shimadzu TOC-L analyzer equipped with an ASI-V autosampler. The concentrations of DOC were calibrated using a six-point calibration curve generated from DOC standards prepared using potassium hydrogen phthalate and UV-oxidized Milli-Q high purity water. The instrumental blank and standard validations for DOC were checked against reference samples of low-carbon water and deep seawater that were provided by Dr. Hansell's Laboratory at the University of Miami, USA. Blank subtraction was carried out using Milli-Q water that was analyzed before each sample. The average blank associated with DOC measurements was ≤ 4 μM, and the analytic precision on triplicate injections was ± 3%. All DOC samples were analyzed in duplicate, and the standard deviations of the replicate measurements ranged from ± 0.1 to 4.0 μM.

For Δ^{14}C-DOC measurements, seawater samples were UV-oxidized and extracted as gaseous CO_2 using a previously described modified method (Xue et al., 2015). Briefly, following the UV-oxidation of DOC, the generated CO_2 was purged and collected with ultrahigh purity helium gas through the vacuum line cryogenically and flame-sealed inside a 6 mm OD quartz tube. The oxidization efficiency that was tested using a DOC standard solution (oxalic acid) was ~ 95% (Xue et al., 2015). Both the δ^{13}C and Δ^{14}C were measured at the National Ocean Sciences Accelerator Mass Spectrometry (NOSAMS) facility at the Woods Hole Oceanography Institution (WHOI). The gaseous CO_2 was split into a small fraction for δ^{13}C measurement using a VG isotope ratio mass spectrometer, and the rest was graphitized for Δ^{14}C analysis using accelerator mass spectrometry. Radiocarbon results were reported as modern fraction (McNichol et al., 1994), and δ^{13}C values were reported in ‰ relative to the Vienna Pee Dee Belemnite (VPDB) standard. The analytic precision for δ^{13}C is <0.2‰, and the error of Δ^{14}C measurement is ±5‰, as determined from the standard.

Results

Hydrographic characteristics

The hydrographic data (temperature and salinity) are listed in Supplementary Table S1, and the vertical profiles are plotted in Figure 2. The characteristics of the water are further described in the *T-S* diagram (Figure 3A). The water temperature was higher at the surface (5 m: 26.8-30.8°C), decreased with depth down to approximately 1,500 m (2.7° C), and then remained constant at depths below 1,500 m at

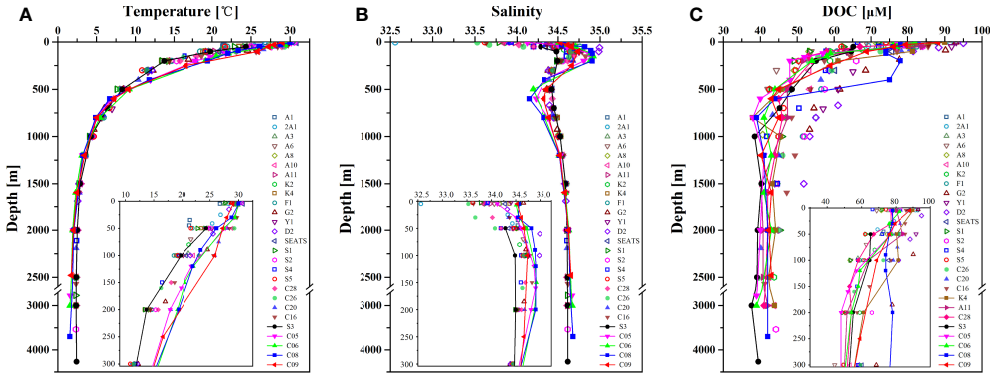

FIGURE 2
Depth profiles of **(A)** water temperature, **(B)** salinity, and **(C)** DOC concentrations measured at the 27 stations in the northern SCS and western NP during three cruises in 2015, 2016 and 2019 in this study and a previous report, as described in Figure 1. The depth below 2,500 m is on a different scale, and the inset figures show profiles in the upper 300 m depth. Note that the hydrographic data and DOC concentrations for eight stations (S1, S2, S3, D2, A11, K2, C05 and C08) were collected on the same cruises and have been previously published (Ding et al., 2020). These data are cited for comparison with the 19 stations in this study.

density levels of σ_0 ≥27.6 kg/m^3 at all stations (Figures 2A, 3A). The salinity ranged from 32.56 to 34.99 and exhibited a profile trend that was opposite to that of temperature (Figure 2B), i.e., lower at the surface (5 m: 32.56-34.65), increasing rapidly with depth to a maximum at a water depth of approximately 60-200 m (at a density range of 23.1-25.2 σ_0) and decreasing again to a minimum at a water depth of approximately 500-600 m (σ_0 ~26.8 kg/m^3). Importantly, the salinity maximum and minimum values were significantly weakened in the northern SCS compared to those in the western NP (i.e., stations C05, C06 and C08). The salinity remained relatively homogeneous below 1,500 m (at σ_0 ≥27.6 kg/m^3) for all stations (Figures 2B, 3A). The abnormally lower surface salinity (S=32.56) at station 2A1, which was sampled after heavy rainfall, should be noted. In contrast, as shown in the *T-S* diagram (Figure 3A), a less curved inverse "*S*" shape of the *T-S* property was observed in the northern SCS (i.e., stations S3, A10 and C26).

Concentrations and distribution of DOC

At the 27 stations sampled on the three cruises in this study and in a previous study (Ding et al., 2020), the concentrations of DOC varied within a range of 38-95 μM for the spring and summer seasons of 2015-2016 and 2019 in the northern SCS and western NP (Figure 2C and Table S1). High DOC concentrations (66-95 μM) were measured in the upper 20 m of the water column (σ_0 < 22.3; Figures 2C, 3B), especially at the 2A1 shelf station and at stations (D2, Y1, G2 and F1) (91-95 μM) near southwestern Taiwan and the western Luzon Strait region. The DOC concentrations decreased rapidly down to a depth of approximately 800 m and then remained relatively low and constant in a range of 38-45 μM below a 2,000 m depth at a density σ_0 > 27.6 across all stations (Figures 2C, 3B). The average DOC concentrations below a 1,500 depth at most stations (except S4 and D2) were similar within analytic error, ranging from 39 ± 1 μM (S3) to 44 ± 3 μM (C16), compared well to the concentrations in the deep western NP (39-43 μM, average 41 ± 2 μM). As plotted in Figures 2C, 3B, the DOC concentrations showed large spatial variations above the 100 m water depth (at σ_0 ≤ 24.9) among the stations, with visibly higher values (78-95 μM) at stations (D2, Y1, G2, F1, C16 and C20) near southwestern Taiwan and the western Luzon Strait than at stations S1, A6, A8 and C28 (53-77 μM).

Degradation of DOC at SEATS

In the laboratory incubation experiments, when the surface water (5 m) in which bacteria were removed was mixed with the water from 700 m and 1500 m depths in which bacteria were present, we observed DOC concentration changes (Table 1 and Figure 4). The measured initial DOC concentrations in the mixed water (71 ± 1 μM and 68 ± 2 μM) were consistent with the calculated DOC concentrations (72 μM and 69 μM) of a simulated mixed water column by diluting surface water DOC (84 μM) with 33% lower DOC water (47 μM) from 700 m, and 33% lower DOC water (41 μM) from 1,500 m, respectively. This indicates that the addition of mesopelagic or deep bacterial inoculum resulted in no notable differences between the *in situ* concentrations and initial DOC concentrations in the incubation (Table 1), and no inadvertent contamination of labile DOC was

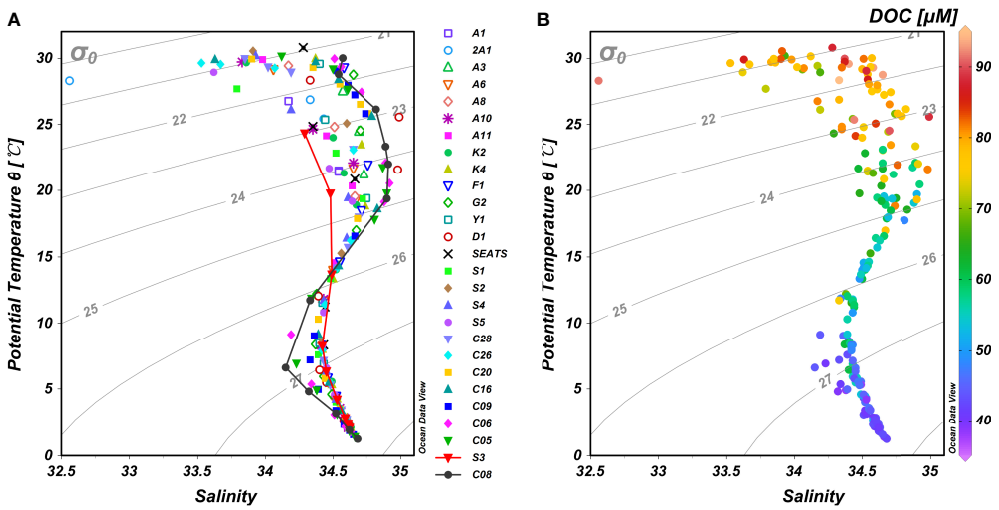

FIGURE 3
Plots of **(A)** potential temperature versus salinity (*T-S*) alone and **(B)** superimposed by observed DOC concentrations at stations in the northern SCS and western NP measured during three cruises (2015, 2016 and 2019). The σ_0 isolines (gray) are included in the figures. The colored symbols in panel **(A)** correspond to CTD data, and solid lines (red and black) designate the representative T-S properties of the SCS and Kuroshio Current at stations S3 and C08, respectively (Ding et al., 2020). All figures were generated using ODV (Schlitzer, 2017).

added during the experimental preparation as suggested previously (Carlson et al., 2004; Li et al., 2021). The DOC concentrations increased to their highest values (76 μM and 73 μM) from the initial concentrations after 25 days and then subsequently decreased with incubation time from 25-180 days (Figure 4). At the end of the incubation (180 days), the initial DOC concentration decreased from 71 μM to 62 μM (Expt. SM521) and from 68 μM to 61 μM (Expt. SD521), and approximately 13% and 10% of the DOC was respired, respectively (Table 1).

The isotopic values measured for DOC at the beginning of and after the incubation experiments also showed noticeable changes. In Expt. SM521 and Expt. SD521, the $\delta^{13}C$ values of DOC decreased from their initial values of -22.3‰ and -22.4‰ to -22.8‰ and -23.1‰, respectively, by the end of the incubation experiments. For the $\Delta^{14}C$ values of DOC, significant decreases of -25‰ and -76‰ were observed in Expt. SM521 and Expt. SD521, respectively, by the end of the incubation experiments (Table 1).

Discussion

Processes that control the concentration and profiles of DOC in the SCS

As the SCS is the largest marginal sea in the western NP, the distribution and dynamics of its DOC could be influenced by many factors, such as primary production, terrestrial inputs from the Pearl River, water exchange with the Kuroshio Current and hydrodynamic mixing of different water masses (Dai et al., 2009; Wu et al., 2015; Meng et al., 2017; Ding et al., 2020; Zhang et al., 2020; Ma et al., 2022). The large variations in the measured DOC concentrations (53-95 μM) above the 100 m water depth were consistent with the results of previous studies (55-97 μM) conducted in the SCS (Pan and Wong, 2015; Wu et al., 2015; Zhang et al., 2020). The surface DOC concentration was notably up to ca. 91 μM at station 2A1, which was sampled after a heavy rain event in early summer near the Pearl River Estuary. Low

TABLE 1 Concentration of DOC and its isotopic values measured at the beginning (Day 0) and end (Day 180) of the two laboratory incubation experiments using seawater collected from the SEATS site.

Experiment ID	Treatment	DOC (μM)		$\delta^{13}C$-DOC (‰)		$\Delta^{14}C$-DOC (‰)	
		Day 0	Day 180	Day 0	Day 180	Day 0	Day 180
SM521	5 m filtrate mixed with unfiltered 700 m seawater	71 ± 1	62 ± 1	-22.3	-22.8	-304	-329
SD521	5 m filtrate mixed with unfiltered 1,500 m seawater	68 ± 2	61 ± 1	-22.4	-23.1	-315	-391

For the two incubation experiments, approximately 6 L of filtered (0.2 μm, to remove bacteria) surface seawater was mixed with 3 L of unfiltered seawater from a 700 m depth (SM521), and 6 L of filtered (0.2 μm) surface seawater was mixed with 3 L of unfiltered seawater from a 1,500 m depth (SD521) within 1 h of seawater collection and filtration.

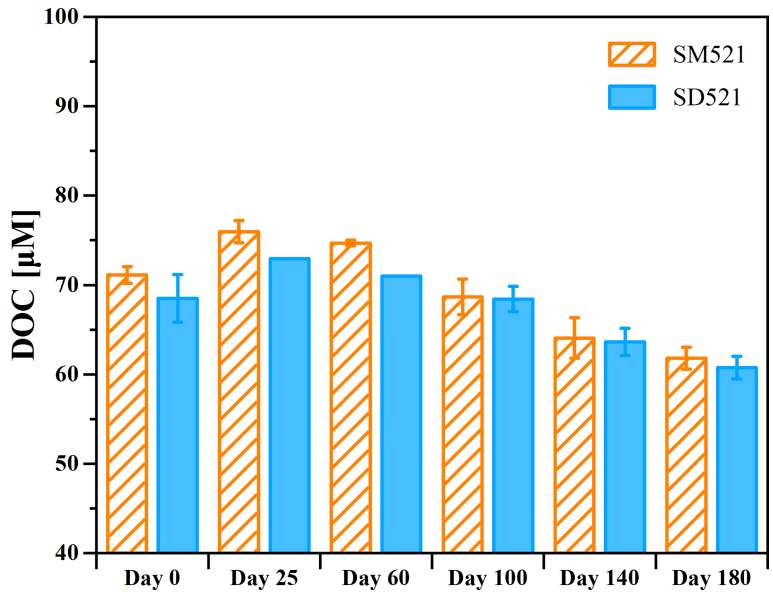

FIGURE 4
Measured DOC concentration changes with time during the two incubation experiments (SM521 and SD521). The error bars denote the means with standard errors from the duplicate analysis.

salinity (S=32.56) water was measured at this station but not at other stations in the study area (Figures 2B, 3A), implying the limited dilution effect of fresh coastal waters. Combined with the low salinity (S=32.56) and high temperature (T=28.3°C) of the surface water, the high DOC concentration at station 2A1 (Figures 2C, 3B) could be modulated by the cross-shelf transport of coastal water. As plotted in Figure 5, significantly high levels of DOC (93-95 μM) were observed in the surface water (≤15 m) at four other stations (D2, G2, F1 and Y1) located near southwestern Taiwan Island and the western Luzon Strait in spring (Figure 5E). At these stations, the salinity in the upper layer was clearly higher than that in the surrounding waters (Figures 5C, D), indicating the intrusion of the Kuroshio Current, which carries high salinity and high DOC water into the region. However, surface DOC concentrations and salinity were not significantly elevated at other stations in the vicinity of the western Luzon Strait in the summer season (stations S1, S5, C16, C20, C26 and C28 in Figures 5D, F). In this context, the intrusion of the Kuroshio Current and the high primary productivity in spring would increase the surface DOC concentrations in the western region of the Luzon Strait. Compared to that in the spring season, the Kuroshio intrusion was weaker in summer and had a limited impact with distance from the Luzon Strait (Du et al., 2013; Nan et al., 2015; Jiang et al., 2020); thus, high surface concentrations were not observed in summer around the same region and at other stations in the SCS basin.

Several studies have used an isopycnal mixing model proposed by Du et al. (2013) to quantify the impact of Kuroshio intrusion on the DOC and chromophoric dissolved organic matter (CDOM) in the upper 100 m water depth of the northern SCS (Wu et al., 2015; Wang et al., 2017; Li et al., 2021). Using this model, we calculated the mixing ratio of the Kuroshio water and SCS water along the isopycnal layer for the *in situ* observed water parcel shown in the *T-S* diagram (Figure 3A). The relative contributions of SCS and Kuroshio water can be derived based on the conservative mixing of salinity or potential temperature (Equations 1-2).

$$R_S\theta_S + R_K\theta_K = \theta \text{ or } R_SS_S + R_KS_K = S \quad (1)$$

$$R_S + R_K = 1 \quad (2)$$

where R_K and R_S denote the Kuroshio and SCS water proportion in the mixed water; S_S, S_K, θ_S *and* θ_K are the end-member values of salinity and potential temperature for the SCS (station S3) and Kuroshio (station C08) water proper in Figure 3A. The station-integrated Kuroshio water fraction (R_{IKW}) were obtained by integrating the Kuroshio water fraction (R_K) over the upper 100 m water column (Figure 6). It appeared that the R_{IKW} in the region near the southwestern Taiwan Island (approximately 0.6) was higher than that in the central northern SCS (< 0.3) in spring (Figure 6A), and both comparable but little higher than that reported in previous studies in the same season (Du et al., 2013; Wu et al., 2015;

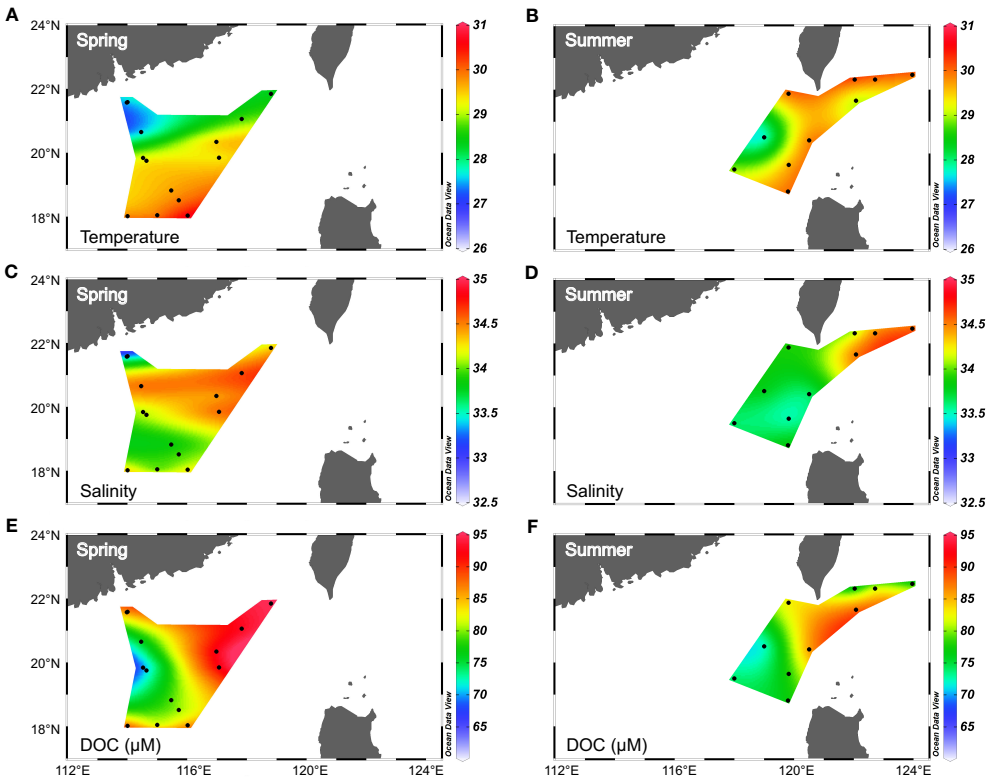

FIGURE 5
Surface distribution (≤15 m water depth) of **(A, B)** temperature (°C), **(C, D)** salinity and **(E, F)** DOC (μM) in the northern SCS and western North Pacific during spring **(A, C, E)** and summer **(B, D, F)** in 2015-2016 and 2019. For comparison, the hydrographic data and DOC concentrations at stations S1, S2, S3, D2, A11, K2, C05 and C08 that were collected during the same three cruises by Ding et al. (2020) are presented. These figures were created using ODV (Schlitzer, 2017).

Wang et al., 2017). During summer, the R_{IKW} was relative lower in the eastern part of the northern SCS with values of approximately 0.2-0.3, excluding the stations C16 and C20 located nearby the Luzon Strait (Figure 6B). The spatial and seasonal distribution of R_{IKW} further support the impact of Kuroshio intrusion on the DOC dynamics in the upper 100 m water depth in the northern SCS.

On the basis of the derived Kuroshio and SCS water fractions (R_K and R_S), DOC concentrations (referred to as DOC_{Model}) along the isopycnal surface due to conservative mixing between

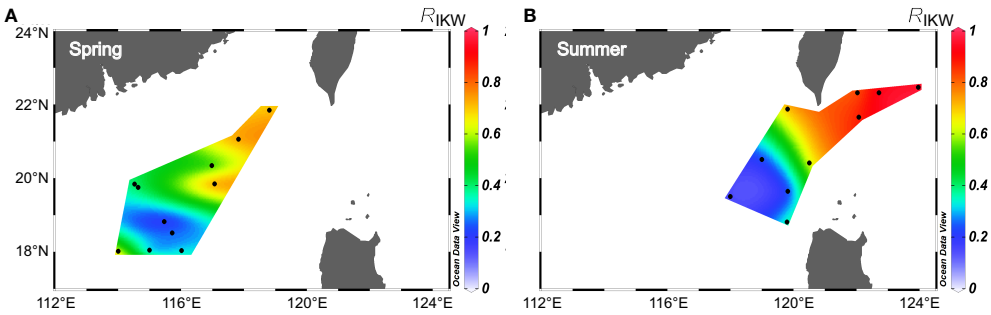

FIGURE 6
Station-integrated Kuroshio water fraction (R_{IKW}) in the upper 100 m of the northern SCS during spring **(A)** and summer **(B)**.

the Kuroshio water proper and SCS water proper can be calculated using Equation 3 (Wu et al., 2015).

$$DOC_{Model} = DOC_S R_S + DOC_K R_K \quad (3)$$

Here, DOC_K and DOC_S are the end-member values of the Kuroshio water (station C08) and SCS water (station S3), respectively. The difference between the field and model calculated DOC concentrations ($\Delta DOC = DOC_{measured} - DOC_{Model}$) could indicate other biologically mediated production (positive ΔDOC value) or degradation (negative ΔDOC value) of DOC in the upper water column. Through this isopycnal mixing model, ΔDOC was estimated in the range of -11 to 10 μM in the upper 100 m of the northern SCS. Therein, the positive ΔDOC values that accounted for approximately 6-14% of the DOC pool at most stations during spring, suggesting a net DOC production. This is consistent with the ~7% increased DOC inventory due to the biological metabolism calculated by Wu et al. (2015) and the fact that the primary production was high in spring (Liu et al., 2002; Liu and Chai, 2009). However, ΔDOC was negative in the upper 50 m at stations S1, S2, S4 and S5 during summer, indicating a net degradation of DOC which accounted for 7-12% of the field DOC pool. The removal of DOC might be attributed to enhanced biodegradation in the mixing zone of SCS and Kuroshio water in summer (Li et al., 2021).

In general, the wide basin of the SCS is oligotrophic year-round and has low primary production due to the low nutrient concentrations and limited influence of Pearl River input (Gong et al., 1992; Lin et al., 2010; Dai et al., 2013). As shown in Figures 2B, 3A, the high salinity signals without freshwater dilution in the slope and basin regions further indicate that the influence of river input was limited in the northern SCS. The DOC depth profiles for the deep stations in the SCS exhibited the same typical vertical patterns as observed in the western NP (stations C05, C06, C08 and C09) and in other open ocean areas with relatively high values (~75 μM) in the surface layer, generally decreased with increasing depth below the euphotic zone by microbial consumption, and then remained low at constant values (~ 40 μM) at greater depths (≥ 1,500 m) and were controlled mainly by hydrodynamic mixing (Carlson et al., 1994; Hansell et al., 2009; Hansell et al., 2012; Druffel and Griffin, 2015; Bercovici and Hansell, 2016). Hung et al. (2007) and Pan and Wong (2015) reported that the distribution of DOC in the northern SCS was largely modulated by physical mixing processes, and the seasonal cycle of surface DOC covaried with temperature rather than primary production, also indicating a physical control on the seasonal variations in DOC. In this respect, we observed a statistically significant negative correlation between DOC and density (σ_t) ($R^2 = 0.82$, $p < 0.001$) at all stations (Figure 7A), suggesting that physical mixing processes played important roles in the distribution and variations in DOC in the northern SCS and western NP. The negative correlation between the DOC and dissolved inorganic carbon (DIC) concentrations (Figure 7B, $R^2 = 0.68$, $p < 0.001$) at the stations also suggested that physical mixing of the water largely influenced the DOC distribution in the northern SCS. However, since DOC is not conservative in the ocean, the observed correlation between DOC and DIC could involve biological and microbial processes (Yang et al., 2016).

Nevertheless, DIC concentrations and Δ^{14}C-DIC could be used as tracers of water mass movement and parcel homogenization as predicted by a solution mixing model and thus supplied evidence of the intensified upwelling and vertical mixing in the water column of the SCS (Ding et al., 2020). To

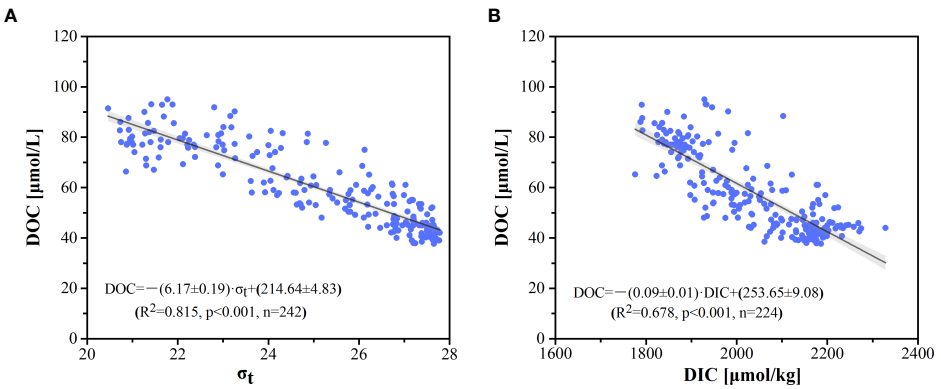

FIGURE 7
Scatterplots of **(A)** DOC concentrations *vs.* density (σ_t) and **(B)** DOC concentrations *vs.* DIC concentrations during the three cruises in the northern SCS and western NP. The solid lines and equations in both plots illustrate the trends of the relationship. The gray areas mark the 95% confidence interval of the linear regression. **(A)** DOC concentrations and the density for all 27 stations were from this study and a previous study; in panel **(B)**, the DIC concentrations were measured at only 25 stations, excluding 2A1 and A10 (Ding et al., 2020 and other unpublished data).

further demonstrate the influence of the physical mixing processes of water on its hydrological and DOC properties, Figure 8 compares the longitudinal distributions of salinity, DOC/DIC concentrations and Δ^{14}C-DIC values for stations across the Luzon Strait. Combined with the *T-S* relationship shown in Figure 3A, the water characteristics in the northern SCS have upwelled and exhibit remarkably weak salinity maximum and minimum values and hence have less curved inverse "*S*" shapes than those in the western NP (Figures 3A, 8A), to which the intensified upwelling and vertical mixing occurring in the SCS might make a significant contribution (Tian et al., 2009; Shu et al., 2014; Wang et al., 2016). In comparison with the chemical parameters at stations C05, C06, C08 and C09 in the western NP, it appeared likely that the deep water in the northern SCS basin, with its low concentrations of DOC and high concentrations and low Δ^{14}C of DIC, upwelled and mixed with the upper water at a depth between 200-500 m, thus diluting the DOC concentrations at stations S1, S5, A11, A10 and K2 (Figures 8B–D). The calculation based on the Δ^{14}C-DIC mass balance revealed that approximately 46-82% of the deep water (≥ 1,500 m) upwelled and mixed with the water in the upper 200-700 m depth (Ding et al., 2020). With the derived deep water fractions, the conservative concentrations of DOC (DOC^0) could be calculated using the same two end-member mixing model. For the end-member values of DOC in the upper 200-500 m depth and deeper waters, we used the average measured DOC concentration of 69 μM in the upper waters and 42 μM in the deep waters in the northern SCS. The DOC^0 could subsequently be calculated within a range of 50-56 μM, which is slightly higher than the measured DOC concentrations (42-53 μM) in the upper 200-500 m depth of the water column at stations S1, S5, A10-A11 and K2 (Figure 8B). The negative ΔDOC values ($DOC_{measured}$ - DOC^0) suggest that net DOC consumption from biological processes could modulate the DOC superimposed on the water physical mixing processes in the northern SCS basin.

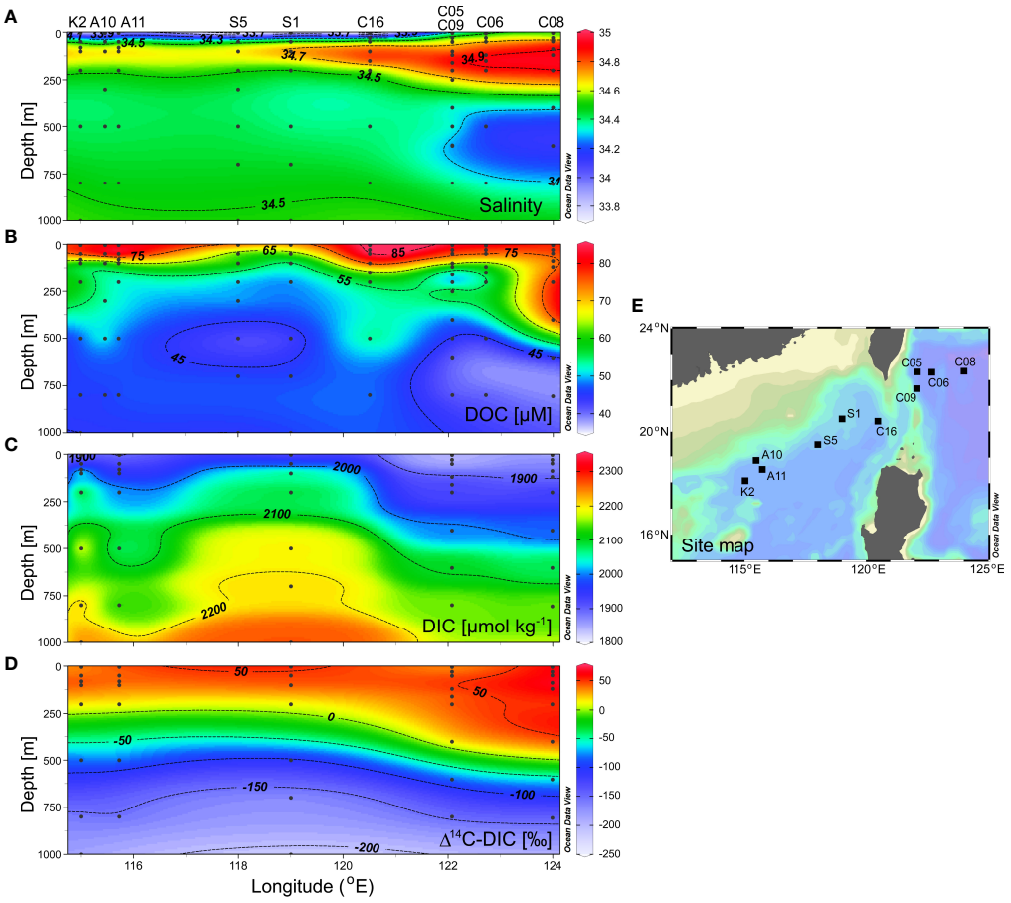

FIGURE 8
Transectional distribution of **(A)** salinity, **(B)** DOC concentrations, **(C)** DIC concentrations and **(D)** Δ^{14}C-DIC values for **(E)** stations sampled from west to the east across the Luzon Strait using ODV (Schlitzer, 2017). Note that DIC concentrations and Δ^{14}C-DIC values are provided for only five stations in panel **(C, D)** due to the lack of data at stations C09, C16, S5 and A10 (Ding et al., 2020).

Given the ΔDOC and the field-measured DOC, we estimated that the bioavailability fraction of DOC in the upper 200-500 m water depth could be in the range of 3-9 μM and account for 6%-20% (average 13 ± 5%) of the total DOC pool at these stations, which was comparable to previous results reported in the slope region of the East China Sea (7%) and the Kuroshio Extension region (8-20%) (Ding et al., 2019).

Below a 1,500 m depth, the DOC concentrations at the stations that were measured during the three cruises were in a narrow range of 42 ± 2 μM, showing no significant difference among stations and seasons, compared to that of 41 ± 2 μM on average at stations in the deep western NP. This deep water DOC appeared to be slightly and unusually enriched (approximately 3-4 μM) in the SCS compared to that found in the NP (39 ± 1 μM) (Feely et al., 2004; Ding et al., 2019; Druffel et al., 2019). The DOC ^{14}C ages in the deep water (≥1,500 m depth) were calculated from Δ^{14}C values at four stations and were plotted against the average deep DOC concentrations of water samples from the northern SCS and other open ocean areas (Figure 9) (Druffel et al., 1992; Druffel and Griffin, 2015; Druffel et al., 2016; Druffel et al., 2019; Ding et al., 2020; Druffel et al., 2021). The ^{14}C ages of the deep DOC in the northern SCS were observed to be close to the ages of the ^{14}C-DOC reported for the deep NP, with values of ~6,000 years (Druffel et al., 2019; Ding et al., 2020; Druffel et al., 2021) (Wang, unpublished data). However, the SCS values departed from the statistical relationship (black line) in the plot shown in Figure 9, also indicating enhanced DOC concentrations at water depths below 1,500 m. The excess DOC in the deep SCS (~ 3-4 μM) we observed was similar to that previously reported by Dai et al. (2009) and Wu et al. (2015). Strong fronts due to the Kuroshio intrusion and interactions with SCS water are associated with enhanced water diapycnal mixing, which could promote distinct lateral transport (Tian et al., 2009; Guo et al., 2017). In addition, a recent study revealed that particles (including sinking and suspended particles) could be laterally transported into the deep SCS and directly provide organic carbon to the dark part of the ocean (Shen et al., 2020). Considering that the residence time of the SCS deep water is less than 30 years (Qu et al., 2006), it is possible that this excess DOC in the deep SCS water results from the breakdown or dissolution of laterally transported particles. Analogously, Lopez and Hansell (2021) also reported deep DOC enrichment within the transitional zone in the NP and suggested that hydrographic fronts could stimulate more carbon export to great depths *via* deep-sinking particles and therefore transfer additional DOC into the deep ocean.

Microbial degradation of DOC

The observed rapid decrease in the DOC concentrations below the euphotic zone in the northern SCS and western NP

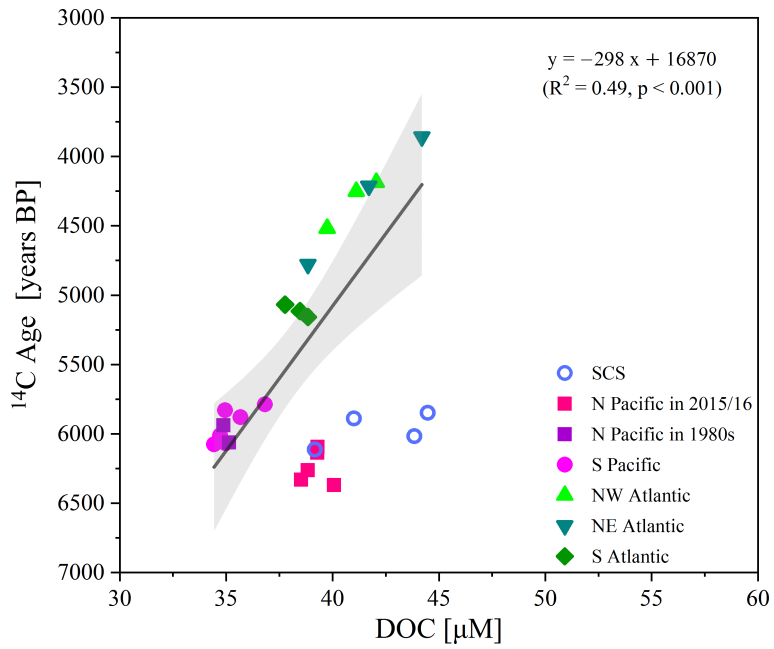

FIGURE 9
Average ^{14}C-DOC ages versus average DOC concentrations at four stations in the northern SCS and in other open ocean sites in the Pacific and Atlantic. Data derived from the SCS (Ding et al., 2020), NP (Druffel et al., 1992; Druffel et al., 2019; Druffel et al., 2021), South Pacific (Druffel and Griffin, 2015; Druffel et al., 2021), and Atlantic (Druffel et al., 2016). The solid line is the Model II geometric mean regression of all points excluding the SCS, and the gray area marks the 95% confidence interval of the linear regression. The equation is also shown in the figure, with a slope of -298 ± 48 and a y-intercept of 16,870 ± 1,832.

clearly indicated that most microbial utilization of DOC took place in the upper water column. For instance, using the changed DOC concentrations in the upper 200 m and the average DOC concentrations (42 μM) below 1,500 m as the background level of refractory DOC in the deep SCS, we calculated the depth distribution of the fractions of labile DOC, semilabile DOC and refractory DOC based on the concentration gradient with depth in the northern SCS. A portion of the surface DOC (approximately 31 ± 5%) was consumed in the upper 200 m depth, which is comparable to the published bioavailable DOC data in the coastal ocean that concluded that bioavailable DOC accounts for 22 ± 12% of the total DOC and the labile DOC fractions (20-40%) of the surface bulk DOC in western North Pacific (Lønborg and Álvarez-Salgado, 2012; Ge et al., 2022). However, most of the DOC, representing 48 to 68% of the surface bulk DOC with a mean value of 54 ± 5%, appeared to be biologically resistant and remained in deep waters in the SCS and western NP.

DOC degradation experiments have been conducted to assess the availability of naturally producing substrates to bacterial assemblages and the corresponding changes in bacterial community structure (Carlson et al., 2004; Nelson and Carlson, 2012; Shen and Benner, 2018; Li et al., 2021). Considering that the labile DOC is largely limited to the euphotic zone (Hansell and Carlson, 2001; Carlson et al., 2010) and based on the depth distribution of the DOC fractions in the northern SCS, the refractory DOC fraction dominated (> 90%) the DOC pool in the 700 m and deeper water layers, indicating that the labile and semilabile DOC only constitutes a small fraction (< 10%, approximately ≤ 5 μM) of the bulk DOC in 700 m and deeper water depth layers. The introduce of labile and semilable DOC from the mesopelagic and deep seawater could be ignored at a volume/volume ratio of 2:1. The results from our incubation experiments demonstrated that DOC produced in the surface water provided a preferential energy source for deep water bacteria. The bioavailable DOC accounted for a relatively small proportion (approximately 10-13%) and was consumed by microbes over 180 days in the incubation experiments (Figure 4). Most of the DOC (≥87%) persisted until the end of the experiments, confirming the current view that most of the DOC is resistant to microbial degradation in the deep ocean (Hansell et al., 2012; Hansell, 2013; Follett et al., 2014; Carlson and Hansell, 2015). However, in a recent study, the bioavailable DOC observed in the treatment of SCS surface filtered seawater inoculated with unfiltered SCS surface seawater was approximately 3 μM and only accounted for a proportion of 5% (Li et al., 2021). In both the two studies, bioavailable DOC is the concentration difference between the initial DOC and the residual DOC at the end of the experiments. The relatively higher bioavailable DOC, therefore, indicated enhanced biodegradations of DOC by the mesopelagic and deep microbes in our experiments, which agrees with the currently accepted assumption that the accumulated DOC at one water depth can become utilized at another depth, although the reasons remain unknown (Carlson et al., 2004; Carlson et al., 2010; Shen and Benner, 2018; Liu et al., 2022). It is interesting to note that the observed increase in DOC concentrations within 25 days was not detected in previous DOC utilization studies (Carlson et al., 2004; Liu et al., 2020). A notable difference among these studies was the incubation temperature, which was room temperature in the present study, while Carlson et al. (2004) and Liu et al. (2020) used the *in situ* temperatures of mesopelagic and deep waters. When the temperature increased from *in situ* to room temperature, little change in the bacterial community could be found (Zhao et al., 2019). In addition, diverse marine microbes have dual roles as producers and consumers of DOC in the ocean (Lechtenfeld et al., 2015; Shen and Benner, 2018). Lechtenfeld et al. (2015) demonstrated that the remaining DOC at the end of their bioassay experiments was directly or indirectly released from bacteria. Considering that factors such as environmental temperature and microbial assemblages impact the ocean carbon cycle, we propose that the DOC released from marine microbes *via* viral lysis, excretion and other processes (Kawasaki and Benner, 2006; Moran et al., 2022) is expected to increase with increasing environmental temperature during the initial 25 days of incubation. This hypothesis, however, needs to be tested in future research. Nevertheless, the increased DOC within 25 days may also contribute to the enhanced biodegradation of DOC, which is analogous to the priming effect observed when the labile substrates added and increased the removal of DOC in previous bioassay experiments (Shen and Benner, 2020).

It can be clearly seen that the isotopic composition of DOC (both ^{13}C and ^{14}C) varied significantly during the incubation experiments. The remaining DOC at the end of the incubations had more depleted ^{14}C values (-329‰ and -391‰) than did the original DOC (-304‰ and -315‰), but these values were approximately 150‰ higher than the $\Delta^{14}C$-DOC values in the deep SCS (average -525 ± 15‰). This indicated that the removal of DOC that was characterized by these enriched ^{14}C values occurred in the water after 180 days of incubation. Our observations agree with previous studies showing that open-ocean bacteria preferentially assimilated modern components of DOC and were enriched in ^{14}C relative to bulk DOC (Cherrier et al., 1999). Additionally, the $\delta^{13}C$-DOC values at the end of the incubation period were slightly lighter (-0.5‰ and -0.7‰, respectively) than the original values, but all were within the range of -20.5‰ to -23.5‰ that was recently reported for DOC in the SCS and in other open ocean areas (Druffel et al., 2019; Ding et al., 2020; Druffel et al., 2021). The variations in $\delta^{13}C$-DOC values after 180 days of incubation in a closed system indicated that part of the enriched ^{13}C constituents of marine autochthonous DOC could be preferentially removed in the microbial degradation processes, leaving behind DOC with depleted ^{13}C constituents, thus resulting in the residual DOC being relatively depleted in $\delta^{13}C$ (-22.8‰ to -23.1‰). This finding on the DOC isotopic composition changes ($\Delta^{14}C$-DOC and $\delta^{13}C$-DOC) supports the variations in the DOC concentrations discussed above, where recently produced and accumulated DOC can become utilized at

deeper water depth, although it was not available for microbial utilization at the upper depth.

Conclusion

The results of our study indicate that the DOC concentrations ranged from 38 to 95 μM in the shelf-slope-basin regions of the northern SCS and western NP in the spring and summer seasons. The large spatial variations in DOC (53 to 95 μM) in the upper 100 m among the shelf-slope-basin regions in the northern SCS were influenced by a combination of factors, including primary production, terrestrial inputs from the Pearl River and the intrusion of the Kuroshio Current. Compared with the DOC concentrations in the western NP, the diluted DOC concentrations at a mesopelagic depth in the northern SCS basin reflect the primary influence of the mixing process of upwelled deep water. Compared with the DOC levels in the deep Pacific and South Atlantic Oceans, a slight excess of DOC concentrations (~ 3-4 μM) was observed in the deep water of the SCS.

The results of these incubation experiments indicated that 10-20% of the surface DOC was consumed by mesopelagic and/or deep water bacteria. A distinct change in the isotopic compositions of DOC (Δ^{14}C-DOC and δ^{13}C-DOC values) was also simultaneously identified along with shifts in DOC concentrations in response to DOC degradation, indicating that modern and enriched $^{14}C/^{13}C$ constituents of DOC are preferentially removed in the ocean.

Data availability statement

The original contributions presented in the study are included in the article/Supplementary Material. Further inquiries can be directed to the corresponding author.

Author contributions

LD and SS collected samples, participated in the sample analysis and data process. CL analyzed the DOC samples. LD wrote the manuscript. XW designed the study and edited the manuscript. All authors provided intellectual input for data interpretation and contributed to the article and approved the submitted version.

Funding

Financial support for this work was provided by the Ocean Program of the National Natural Science Foundation of China (Grant numbers 91858210 and 91428101).

Acknowledgments

We thank Yuanzhi Qi and Hongmei Zhang for assistance with sample analysis in the laboratory. We also express our thanks to the captains and crew members of R/V *Shiyan 3*, R/V *Dongfanghong 2* and R/V *Haida* for their help during the cruises.

Conflict of interest

The authors declare that the research was conducted in the absence of any commercial or financial relationships that could be construed as a potential conflict of interest.

Publisher's note

All claims expressed in this article are solely those of the authors and do not necessarily represent those of their affiliated organizations, or those of the publisher, the editors and the reviewers. Any product that may be evaluated in this article, or claim that may be made by its manufacturer, is not guaranteed or endorsed by the publisher.

Supplementary material

The Supplementary Material for this article can be found online at: https://www.frontiersin.org/articles/10.3389/fmars.2022.973694/full#supplementary-material

References

Azam, F., and Worden, A. Z. (2004). Microbes, molecules, and marine ecosystems. *Science* 303, 1622–1624. doi: 10.1126/science.1093892

Benner, R., and Amon, R. M. W. (2015). The size-reactivity continuum of major bioelements in the ocean. *Annu. Rev. Mar. Sci.* 7, 185–205. doi: 10.1146/annurev-marine-010213-135126

Bercovici, S. K., and Hansell, D. A. (2016). Dissolved organic carbon in the deep southern ocean: Local versus distant controls. *Global Biogeochem. Cycles* 30, 350–360. doi: 10.1002/2015GB005252

Carlson, C. A., and Ducklow, H. W. (1996). Growth of bacterioplankton and consumption of dissolved organic carbon in the Sargasso Sea. *Aquat. Microb. Ecol.* 10, 69–85. doi: 10.3354/ame010069

Carlson, C. A., Ducklow, H. W., Hansell, D. A., and Smith, W. O. (1998). Organic carbon partitioning during spring phytoplankton blooms in the Ross Sea polynya and the Sargasso Sea. *Limnol. Oceanogr.* 43, 375–386. doi: 10.4319/lo.1998.43.3.0375

Carlson, C. A., Ducklow, H. W., and Michaels, A. F. (1994). Annual flux of dissolved organic carbon from the euphotic zone in the northwestern Sargasso Sea. *Nature* 371, 405–408. doi: 10.1038/371405a0

Carlson, C. A., Ducklow, H. W., and Sleeter, T. D. (1996). Stocks and dynamics of bacterioplankton in the northwestern Sargasso Sea. *Deep. Sea. Res. Part II Top. Stud. Oceanogr.* 43, 491–515. doi: 10.1016/0967-0645(95)00101-8

Carlson, C. A., Giovannoni, S. J., Hansell, D. A., Goldberg, S. J., Parsons, R., and Vergin, K. (2004). Interactions among dissolved organic carbon, microbial processes, and community structure in the mesopelagic zone of the northwestern Sargasso Sea. *Limnol. Oceanogr.* 49, 1073–1083. doi: 10.4319/lo.2004.49.4.1073

Carlson, C. A., and Hansell, D. A. (2015). "DOM sources, sinks, reactivity, and budgets," in *Biogeochemistry of marine dissolved organic matter, 2nd ed.* Eds. D. A. Hansell and C. A. Carlson (San Diego: Academic Press), 65–126.

Carlson, C. A., Hansell, D. A., Nelson, N. B., Siegel, D. A., Smethie, W. M., Khatiwala, S., et al. (2010). Dissolved organic carbon export and subsequent remineralization in the mesopelagic and bathypelagic realms of the north Atlantic basin. *Deep. Sea. Res. Part II* 57, 1433–1445. doi: 10.1016/j.dsr2.2010.02.013

Chen, C. T. A., Wang, S. L., Wang, B. J., and Pai, S. C. (2001). Nutrient budgets for the south China Sea basin. *Mar. Chem.* 75, 281–300. doi: 10.1016/S0304-4203(01)00041-X

Cherrier, J., Bauer, J. E., and Druffel, E. R. M. (1996). Utilization and turnover of labile dissolved organic matter by bacterial heterotrophs in eastern north pacific surface waters. *Mar. Ecol. Prog. Ser.* 139, 267–279. doi: 10.3354/meps139267

Cherrier, J., Bauer, J. E., Druffel, E. R. M., Coffin, R. B., and Chanton, J. P. (1999). Radiocarbon in marine bacteria: Evidence for the ages of assimilated carbon. *Limnol. Oceanogr.* 44, 730–736. doi: 10.4319/lo.1999.44.3.0730

Dai, M., Cao, Z., Guo, X., Zhai, W., Liu, Z., Yin, Z., et al. (2013). Why are some marginal seas sources of atmospheric CO_2? *Geophys. Res. Lett.* 40, 2154–2158. doi: 10.1002/grl.50390

Dai, M. H., Gan, J., Han, A., Kung, H. S., and Yin, Z. (2014). "Physical dynamics and biogeochemistry of the pearl river plume," in *Biogeochemical dynamics at major river-coastal interfaces. linkages with global change.* Eds. T. S. Bianchi, M. Allison and W.-J. Cai (New York: Cambridge University Press), 321–352.

Dai, M., Meng, F., Tang, T., Kao, S.-J., Lin, J., Chen, J., et al. (2009). Excess total organic carbon in the intermediate water of the south China Sea and its export to the north pacific. *Geochem. Geophys. Geosyst.* 10, Q12002. doi: 10.1029/2009GC002752

Ding, L., Ge, T., and Wang, X. (2019). Dissolved organic carbon dynamics in the East China Sea and the northwest pacific ocean. *Ocean. Sci.* 15, 1177–1190. doi: 10.5194/os-15-1177-2019

Ding, L., Qi, Y., Shan, S., Ge, T., Luo, C., and Wang, X. (2020). Radiocarbon in dissolved organic and inorganic carbon of the south China Sea. *J. Geophys. Res. Ocean.* 125, e2020JC016073. doi: 10.1029/2020JC016073

Druffel, E. R. M., and Griffin, S. (2015). Radiocarbon in dissolved organic carbon of the south pacific ocean. *Geophys. Res. Lett.* 42, 4096–4101. doi: 10.1002/2015GL063764

Druffel, E. R. M., Griffin, S., Coppola, A. I., and Walker, B. D. (2016). Radiocarbon in dissolved organic carbon of the Atlantic ocean. *Geophys. Res. Lett.* 43, 5279–5286. doi: 10.1002/2016GL068746

Druffel, E. R. M., Griffin, S., Lewis, C. B., Rudresh, M., Garcia, N. G., Key, R. M., et al. (2021). Dissolved organic radiocarbon in the eastern pacific and southern oceans. *Geophys. Res. Lett.* 48, e2021GL092904. doi: 10.1029/2021GL092904

Druffel, E. R. M., Griffin, S., Wang, N., Garcia, N. G., McNichol, A. P., Key, R. M., et al. (2019). Dissolved organic radiocarbon in the central pacific ocean. *Geophys. Res. Lett.* 46, 5396–5403. doi: 10.1029/2019GL083149

Druffel, E. R. M., Williams, P. M., Bauer, J. E., and Ertel, J. R. (1992). Cycling of dissolved and particulate organic matter in the open ocean. *J. Geophys. Res.* 97, 15639–15659. doi: 10.1029/92JC01511

Ducklow, H. W. (1999). The bacterial component of the oceanic euphotic zone. *FEMS Microbiol. Ecol.* 30, 1–10. doi: 10.1016/S0168-6496(99)00031-8

Du, C., Liu, Z., Dai, M., Kao, S. J., Cao, Z., Zhang, Y., et al. (2013). Impact of the kuroshio intrusion on the nutrient inventory in the upper northern south China Sea: insights from an isopycnal mixing model. *Biogeosciences* 10, 6419–6432. doi: 10.5194/bg-10-6419-2013

Feely, R. A., Dichson, D., Hansell, D. A., and Carlson, C. A. (2004) *Carbon dioxide, hydrographic, and chemical data obtained during the R/V Melville cruise in the pacific ocean on CLIVAR repeat hydrography sections P02_2004 (15 June - 27 august, 2004).* Available at: http://cdiac.ornl.gov/ftp/oceans/CLIVAR/P02_2004.data/.

Fenchel, T. (2008). The microbial loop-25 years later. *J. Exp. Mar. Bio. Ecol.* 366, 99–103. doi: 10.1016/j.jembe.2008.07.013

Follett, C. L., Repeta, D. J., Rothman, D. H., Xu, L., and Santinelli, C. (2014). Hidden cycle of dissolved organic carbon in the deep ocean. *Proc. Natl. Acad. Sci. U.S.A.* 111, 16706–16711. doi: 10.1073/pnas.1407445111

Ge, T., Luo, C., Ren, P., Zhang, H., Chen, H., Chen, Z., et al. (2022). Dissolved organic carbon along a meridional transect in the western north pacific ocean: Distribution, variation and controlling processes. *Front. Mar. Sci.* 9. doi: 10.3389/fmars.2022.909148

Gong, G. C., Liu, K. K., Liu, C. T., and Pai, S. C. (1992). The chemical hydrography of the south China Sea west of Luzon and a comparison with the West Philippine Sea. *Terr. Atmos. Ocean. Sci.* 3, 587–602. doi: 10.3319/TAO.1992.3.4.587(O

Guo, L., Santschi, P. H., Cifuentes, L. A., Trumbore, S. E., and Southon, J. (1996). Cycling of high-molecular-weight dissolved organic matter in the middle Atlantic bight as revealed by carbon isotopic (^{13}C and ^{14}C) signatures. *Limnol. Oceanogr.* 41, 1242–1252. doi: 10.4319/lo.1996.41.6.1242

Guo, L., Xiu, P., Chai, F., Xue, H., Wang, D., and Sun, J. (2017). Enhanced chlorophyll concentrations induced by kuroshio intrusion fronts in the northern south China Sea. *Geophys. Res. Lett.* 44, 11565–11572. doi: 10.1002/2017GL075336

Hansell, D. A. (2013). Recalcitrant dissolved organic carbon fractions. *Annu. Rev. Mar. Sci.* 5, 421–445. doi: 10.1146/annurev-marine-120710-100757

Hansell, D. A., and Carlson, C. A. (1998). Net community production of dissolved organic carbon. *Global Biogeochem. Cycles* 12, 443–453. doi: 10.1029/98gb01928

Hansell, D. A., and Carlson, C. A. (2001). Marine dissolved organic matter and the carbon cycle. *Oceanography* 14, 41–49. doi: 10.5670/oceanog.2001.05

Hansell, D. A., Carlson, C. A., Repeta, D. J., and Schlitzer, R. (2009). Dissolved organic matter in the ocean: A controversy stimulates new insights. *Oceanography* 22, 202–211. doi: 10.5670/oceanog.2009.109

Hansell, D. A., Carlson, C. A., and Schlitzer, R. (2012). Net removal of major marine dissolved organic carbon fractions in the subsurface ocean. *Global Biogeochem. Cycles* 26, GB1016. doi: 10.1029/2011gb004069

Hansell, D. A., Carlson, C. A., and Suzuki, Y. (2002). Dissolved organic carbon export with north pacific intermediate water formation. *Global Biogeochem. Cycles* 16, 1007. doi: 10.1029/2000GB001361

Hung, J. J., Wang, S. M., and Chen, Y. L. (2007). Biogeochemical controls on distributions and fluxes of dissolved and particulate organic carbon in the northern south China Sea. *Deep. Sea. Res. Part II Top. Stud. Oceanogr.* 54, 1486–1503. doi: 10.1016/j.dsr2.2007.05.006

Jiang, Y., Zhang, S., Tian, J., Zhang, Z., Gan, J., and Wu, C.-R. (2020). An examination of circulation characteristics in the Luzon strait and the south China Sea using high-resolution regional atmosphere-ocean coupled models. *J. Geophys. Res. Ocean.* 125, e2020JC016253. doi: 10.1029/2020JC016253

Kawasaki, N., and Benner, R. (2006). Bacterial release of dissolved organic matter during cell growth and decline: Molecular origin and composition. *Limnol. Oceanogr.* 51, 2170–2180. doi: 10.4319/lo.2006.51.5.2170

Kirchman, D. L., Suzuki, Y., Garside, C., and Ducklow, H. W. (1991). High turnover rates of dissolved organic carbon during a spring phytoplankton bloom. *Nature* 352, 612–614. doi: 10.1038/352612a0

Lønborg, C., and Álvarez-Salgado, X. A. (2012). Recycling versus export of bioavailable dissolved organic matter in the coastal ocean and efficiency of the continental shelf pump. *Global Biogeochem. Cycles* 26, GB3018. doi: 10.1029/2012gb004353

Lechtenfeld, O. J., Hertkorn, N., Shen, Y., Witt, M., and Benner, R. (2015). Marine sequestration of carbon in bacterial metabolites. *Nat. Commun.* 6, 6711. doi: 10.1038/ncomms7711

Li, X., Wu, K., Gu, S., Jiang, P., Li, H., Liu, Z., et al. (2021). Enhanced biodegradation of dissolved organic carbon in the western boundary kuroshio current when intruded to the marginal south China Sea. *J. Geophys. Res. Ocean.* 126, e2021JC017585. doi: 10.1029/2021JC017585

Lin, I.-I., Lien, C.-C., Wu, C.-R., Wong, G. T. F., Huang, C.-W., and Chiang, T.-L. (2010). Enhanced primary production in the oligotrophic south China Sea by eddy injection in spring. *Geophys. Res. Lett.* 37, L16602. doi: 10.1029/2010gl043872

Liu, G., and Chai, F. (2009). Seasonal and interannual variability of primary and export production in the south China Sea: a three-dimensional physical-biogeochemical model study. *ICES. J. Mar. Sci.* 66, 420–431. doi: 10.1093/icesjms/fsn219

Liu, K. K., Chao, S. Y., Shaw, P. T., Gong, G. C., Chen, C. C., and Tang, T. Y. (2002). Monsoon-forced chlorophyll distribution and primary production in the south China Sea: observations and a numerical study. *Deep. Sea. Res. Part I* 49, 1387–1412. doi: 10.1016/S0967-0637(02)00035-3

Liu, S., Longnecker, K., Kujawinski, E. B., Vergin, K., Bolaños, L. M., Giovannoni, S. J., et al. (2022). Linkages among dissolved organic matter export, dissolved metabolites, and associated microbial community structure response in the northwestern Sargasso Sea on a seasonal scale. *Front. Microbiol.* 13. doi: 10.3389/fmicb.2022.833252

Liu, S., Parsons, R., Opalk, K., Baetge, N., Giovannoni, S., Bolaños, L. M., et al. (2020). Different carboxyl-rich alicyclic molecules proxy compounds select distinct bacterioplankton for oxidation of dissolved organic matter in the mesopelagic Sargasso Sea. *Limnol. Oceanogr.* 65, 1532–1553. doi: 10.1002/lno.11405

Loh, A. N., Bauer, J. E., and Druffel, E. R. (2004). Variable ageing and storage of dissolved organic components in the open ocean. *Nature* 430, 877–881. doi: 10.1038/nature02780

Lopez, C. N., and Hansell, D. A. (2021). Evidence of deep DOC enrichment *via* particle export beneath subarctic and northern subtropical fronts in the north pacific. *Front. Mar. Sci.* 8. doi: 10.3389/fmars.2021.659034

Ma, W., Xiu, P., Yu, Y., Zheng, Y., and Chai, F. (2022). Production of dissolved organic carbon in the south China Sea: A modeling study. *Sci. China Earth Sci.* 65, 351–364. doi: 10.1007/s11430-021-9817-2

McNichol, A. P., Jones, G. A., Hutton, D. L., Gagnon, A. R., and Key, R. M. (1994). The rapid preparation of seawater ΣCO_2 for radiocarbon analysis at the national ocean sciences AMS facility. *Radiocarbon* 36, 237–246. doi: 10.1017/S0033822200040522

Meng, F., Dai, M., Cao, Z., Wu, K., Zhao, X., Li, X., et al. (2017). Seasonal dynamics of dissolved organic carbon under complex circulation schemes on a large continental shelf: The northern south China Sea. *J. Geophys. Res. Ocean.* 122, 9415–9428. doi: 10.1002/2017jc013325

Moran, M. A., Kujawinski, E. B., Schroer, W. F., Amin, S. A., Bates, N. R., Bertrand, E. M., et al. (2022). Microbial metabolites in the marine carbon cycle. *Nat. Microbiol.* 7, 508–523. doi: 10.1038/s41564-022-01090-3

Nan, F., Xue, H., and Yu, F. (2015). Kuroshio intrusion into the south China Sea: A review. *Prog. Oceanogr.* 137 (Part A), 314–333. doi: 10.1016/j.pocean.2014.05.012

Nelson, C. E., and Carlson, C. A. (2012). Tracking differential incorporation of dissolved organic carbon types among diverse lineages of Sargasso Sea bacterioplankton. *Environ. Microbiol.* 14, 1500–1516. doi: 10.1111/j.1462-2920.2012.02738.x

Pan, X., and Wong, G. T. F. (2015). An improved algorithm for remotely sensing marine dissolved organic carbon: Climatology in the northern south China Sea shelf-sea and adjacent waters. *Deep. Sea. Res. Part II* 117, 131–142. doi: 10.1016/j.dsr2.2015.02.025

Qu, T., Girton, J. B., and Whitehead, J. A. (2006). Deepwater overflow through Luzon strait. *J. Geophys. Res. Ocean.* 111, C01002. doi: 10.1029/2005jc003139

Repeta, D. J. (2015). "Chemical characterization and cycling of dissolved organic matter," in *Biogeochemistry of marine dissolved organic matter, 2nd ed*. Eds. D. A. Hansell and C. A. Carlson (San Diego: Academic Press), 21–63.

Repeta, D. J., and Aluwihare, L. I. (2006). Radiocarbon analysis of neutral sugars in high-molecular-weight dissolved organic carbon: Implications for organic carbon cycling. *Limnol. Oceanogr.* 51, 1045–1053. doi: 10.4319/lo.2006.51.2.1045

Riedel, T., and Dittmar, T. (2014). A method detection limit for the analysis of natural organic matter *via* Fourier transform ion cyclotron resonance mass spectrometry. *Anal. Chem.* 86, 8376–8382. doi: 10.1021/ac501946m

Schlitzer, R. (2017) *Ocean data view*. Available at: http://odv.awi.de.

Sharp, J. H., Benner, R., Bennett, L., Carlson, C. A., Fitzwater, S. E., Peltzer, E. T., et al. (1995). Analyses of dissolved organic carbon in seawater: The JGOFS EqPac methods comparison. *Mar. Chem.* 48, 91–108. doi: 10.1016/0304-4203(94)00040-K

Shen, Y., and Benner, R. (2018). Mixing it up in the ocean carbon cycle and the removal of refractory dissolved organic carbon. *Sci. Rep.* 8, 2542. doi: 10.1038/s41598-018-20857-5

Shen, Y., and Benner, R. (2020). Molecular properties are a primary control on the microbial utilization of dissolved organic matter in the ocean. *Limnol. Oceanogr.* 65, 1061–1071. doi: 10.1002/lno.11369

Shen, J., Jiao, N., Dai, M., Wang, H., Qiu, G., Chen, J., et al. (2020). Laterally transported particles from margins serve as a major carbon and energy source for dark ocean ecosystems. *Geophys. Res. Lett.* 47, e2020GL088971. doi: 10.1029/2020GL088971

Shu, Y., Xue, H., Wang, D., Chai, F., Xie, Q., Yao, J., et al. (2014). Meridional overturning circulation in the south China Sea envisioned from the high-resolution global reanalysis data GLBa0.08. *J. Geophys. Res. Ocean.* 119, 3012–3028. doi: 10.1002/2013JC009583

Tian, J. W., Yang, Q. X., and Zhao, W. (2009). Enhanced diapycnal mixing in the south China Sea. *J. Phys. Oceanogr.* 39, 3191–3203. doi: 10.1175/2009JPO3899.1

Varela, M., Rodríguez-Ramos, T., Guerrero-Feijóo, E., and Nieto-Cid, M. (2020). Changes in activity and community composition shape bacterial responses to size-fractionated marine DOM. *Front. Microbiol.* 11. doi: 10.3389/fmicb.2020.586148

Walker, B. D., Beaupré, S. R., Guilderson, T. P., Druffel, E. R. M., and McCarthy, M. D. (2011). Large-Volume ultrafiltration for the study of radiocarbon signatures and size vs. age relationships in marine dissolved organic matter. *Geochim. Cosmochim. Acta* 75, 5187–5202. doi: 10.1016/j.gca.2011.06.015

Walker, B. D., Primeau, F. W., Beaupré, S. R., Guilderson, T. P., Druffel, E. R. M., and McCarthy, M. D. (2016). Linked changes in marine dissolved organic carbon molecular size and radiocarbon age. *Geophys. Res. Lett.* 43, 10385–10393. doi: 10.1002/2016GL070359

Wang, C., Guo, W., Li, Y., Stubbins, A., Li, Y., Song, G., et al. (2017). Hydrological and biogeochemical bontrols on absorption and fluorescence of dissolved organic matter in the northern south China Sea. *J. Geophys. Res. Biogeosci.* 122, 3405–3418. doi: 10.1002/2017JG004100

Wang, P., and Li, Q. (2009). "Oceanographical and geological background," in *The south China Sea: Paleoceanography and sedimentology*. Eds. P. Wang and Q. Li (Netherlands: Springer), 25–73.

Wang, D., Xiao, J., Shu, Y., Xie, Q., Chen, J., and Wang, Q. (2016). Progress on deep circulation and meridional overturning circulation in the south China Sea. *Sci. China Earth Sci.* 59, 1827–1833. doi: 10.1007/s11430-016-5324-6

Wu, K., Dai, M., Chen, J., Meng, F., Li, X., Liu, Z., et al. (2015). Dissolved organic carbon in the south China Sea and its exchange with the Western pacific ocean. *Deep. Sea. Res. Part II Top. Stud. Oceanogr.* 122, 41–51. doi: 10.1016/j.dsr2.2015.06.013

Wu, K., Dai, M., Li, X., Meng, F., Chen, J., and Lin, J. (2017). Dynamics and production of dissolved organic carbon in a large continental shelf system under the influence of both river plume and coastal upwelling. *Limnol. Oceanogr.* 62, 973–988. doi: 10.1002/lno.10479

Xue, Y., Ge, T., and Wang, X. (2015). An effective method of UV-oxidation of dissolved organic carbon in natural waters for radiocarbon analysis by accelerator mass spectrometry. *J. Ocean. Univ. China* 14, 989–993. doi: 10.1007/s11802-015-2935-z

Yang, L., Chen, C.-T. A., Lui, H.-K., Zhuang, W.-E., and Wang, B.-J. (2016). Effects of microbial transformation on dissolved organic matter in the east Taiwan strait and implications for carbon and nutrient cycling. *Estuar. Coast. Shelf. Sci.* 180, 59–68. doi: 10.1016/j.ecss.2016.06.021

Zhang, M., Wu, Y., Wang, F., Xu, D., Liu, S., and Zhou, M. (2020). Hotspot of organic carbon export driven by mesoscale eddies in the slope region of the northern south China Sea. *Front. Mar. Sci.* 7. doi: 10.3389/fmars.2020.00444

Zhao, Z., Gonsior, M., Schmitt-Kopplin, P., Zhan, Y., Zhang, R., Jiao, N., et al. (2019). Microbial transformation of virus-induced dissolved organic matter from picocyanobacteria: coupling of bacterial diversity and DOM chemodiversity. *ISME. J.* 13, 2551–2565. doi: 10.1038/s41396-019-0449-1

Ziolkowski, L. A., and Druffel, E. R. M. (2010). Aged black carbon identified in marine dissolved organic carbon. *Geophys. Res. Lett.* 37, L16601. doi: 10.1029/2010GL043963

Zweifel, U. L., Norrman, B., and Hagström, Å. (1993). Consumption of dissolved organic carbon by marine bacteria and demand for inorganic nutrients. *Mar. Ecol. Prog. Ser.* 101, 23–32. doi: 10.3354/MEPS101023